POLARIMETRIC 3-D RECONSTRUCTION FROM MULTICIRCULAR SAR AT P-BAND

Octavio Ponce, Pau Prats, Rolf Scheiber, Andreas Reigber, Alberto Moreira

German Aerospace Center (DLR), Microwaves and Radar Institute
Oberpfaffenhofen, Germany
E-mail: Octavio.Ponce@dlr.de

ABSTRACT

Three-dimensional reconstruction and sub-wavelength resolution can be achieved in Circular SAR (CSAR) mode with a single pass. However, circles or arcs are present when the assumed height during focussing is not that of the target. In 3-D imaging these artifacts are seen as cone-shaped sidelobes due to the poor resolution in the direction perpendicular to the line of sight. In this work, a multicircular fully polarimetric SAR experiment using DLR's F-SAR system at P-band is presented. The purpose is to enhance the resolution while focusing 3-D images by retrieving the backscattering profile in elevation. A phase calibration method using the Singular Value Decomposition (SVD) is presented. Processing methods such as Fast Factorized Back Projection for circular tracks, and reconstruction techniques with coherent averaging with beamforming and compressive sensing for 3-D are used. Finally, the first holographic SAR tomogram at P-Band of a forested area is presented.

***Index Terms*—** Circular SAR, PolSAR, holographic tomography, multicircular SAR, compressive sensing

1. INTRODUCTION

High resolution SAR images in the (x, y) plane and resolution in the vertical plane z can be attained with a single circular pass. However, undesirable sidelobes such as rings or arcs in 2-D and cone-shape figures in 3-D distort the images due to the low resolution in the plane perpendicular to the line-of-sight. The ring-like sidelobes when focusing a 2-D image can be reduced using a Digital Elevation Model (DEM) [1], but not for all targets. This problem can be addressed with the formation of a synthetic aperture in elevation, given the advantage of a very low temporal decorrelation, since circular flights can be done in a relatively short time. 3-D reconstruction with CSAR has been discussed before in [2] at X-band. They propose sparse reconstruction methods that are height-dependent, since their analysis is focused on point-like scatterers. Instead P-band has other advantages like foliage penetration and target detection in forested areas, thus allowing the retrieval of information over $360\,^{\circ}$, similar to holographic tomography [3]. Tomographic research has been done with stripmap SAR at L-band for vegetation studies before [4], [5]. It is intended to show with this paper, the first fully polarimetric multicircular SAR holographic tomogram at P-band of a forested area by exploiting the high resolution attainable in the (x,y,z) volume given by this mode.

In the next section the set-up of a multicircular SAR campaign using the F-SAR system over the region of Vordemwald, Switzerland, is described. Next, a calibration method using the SVD to estimate constant phase errors, is introduced. Then, an overview of the two focusing algorithms used in this work, Fast Factorized Back Projection and 3-D reconstruction using beamforming and Compressive Sensing (CS) for CSAR imaging, is given. Fully polarimetric results of a region of interest are shown and analyzed. This paper finalizes with the conclusions of this work.

2. CIRCULAR SAR CAMPAIGN

The acquired fully polarimetric multicircular SAR data set consists in seven complete circular-like continuous passes obtained at P-band at different altitudes as shown in Fig. 1. The baseline distribution is 40, 40, 60, 60, 80 and 80 m, the mean radius is $\sim$ 3850 m, the transmitted chirp bandwidth is 20 MHz (~ 7.5 m resolution in slant range) and the PRF is 504 Hz. Fig. 2 shows the test region of Vordemwald, Switzerland. It is a forested area and covers a spotlighted region of 2.5 km by 2.5 km. The image is in the Pauli basis (R:HH-VV, G:HV, B:HH+VV), and it was focused using a SRTM as external DEM. Despite the use of this DEM, artifacts such as circles and arcs are present because not all scatterers are focused at the correct height. Targets that are focused at the true height and with an isotropic behaviour show an increment in the resolution due to the circular geometry despite the low bandwidth of the system.

A trihedral corner reflector of 1.5 m was placed in the test scene, pointing to the North ($90\,^{\circ}$). However, it was not possible to install many large corner reflectors to perform the absolute calibration for the full track [5]. Therefore, to correct the phase due to the distance over the whole synthetic aperture, a technique based on the Singular Value Decomposition (SVD) was used.

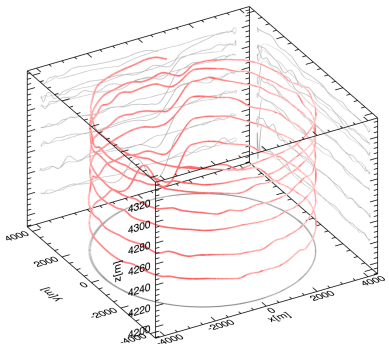

Fig. 1. Circular SAR Campaign, 3-D Tracks, DLR's F-SAR sensor, 2011.

3. HOLOGRAPHIC SAR TOMOGRAPHY RECONSTRUCTION

The cone-shaped sidelobes formed when focusing in 3-D are function of the elevation angle θ_{el} and the slow-time ϕ. Hence, the problem of reducing them should be addressed in subapertures. A synthetic aperture in the vertical direction is used to retrieve the power distribution of the scatterers in elevation. A total o seven circular tracks were flown, while the processing was performed using coherent averaging with beamforming and CS. Moreover, information given by the different polarisations is used to separate scattering mechanisms in height by its polarimetric response. This processing is divided in four stages: focusing of 2-D images in subapertures, phase calibration, focusing of the third dimension in subapertures, and merging of the retrieved energy of all $360\,^{\circ}$ to form the holographic tomogram [5].

Because of efficiency in terms of computational burden, the FFBP was used to focus 2-D images in the slant-range plane in polar coordinates (r, α) every $\phi_{i,j} = 10\,^{\circ}$, where $i = [1..36]$ indicates the subaperture and $j = [1..M]$ the track number. For a given $\phi_{i,j}$ slow-time period, it is assumed that the energy is preserved. As a result of this stage, 36 stacks of M images (M$=$ 7 circular passes) are focused per polarimetric channel (HH-HV-VV). The resolution in the angular and range direction are 2.5 m by 7.5 m, respectively. Due to the fact that there was not available a high resolution DEM for this region, a mean constant height of 550 m was assumed.

High accuracy of the position of the platform in order to integrate the energy of all the circular passes without defocusing is always needed. The accuracy in the phase without calibration was not high enough to retrieve the energy in height, therefore another method using the complex reflectivity of the ground was used. Calibrating the phase without a reflector has been discussed in previous researches [6]. The calibration proposed in this work uses a GPS measured point on ground. This position was used as reference to calibrate

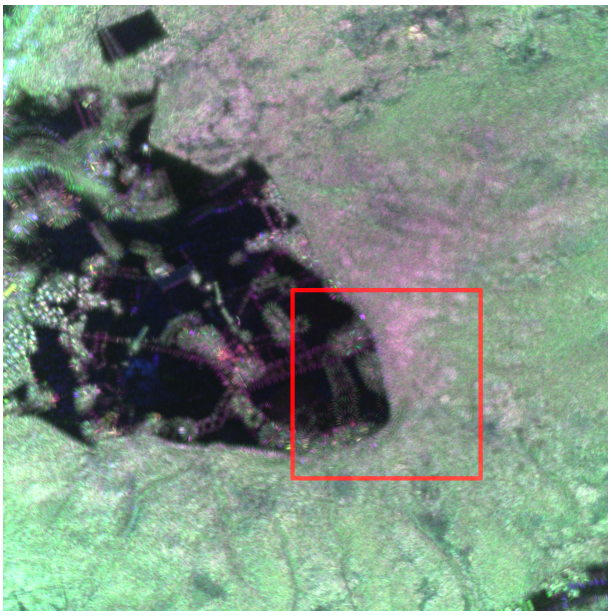

Fig. 2. CSAR image of Vordemwald, Switzerland, 2.5 km x 2.5 km, 0.25 m x 0.25 m sampling, $360\,^{\circ}$ integration processing, Pauli decomposition, red square: region of interest.

constant errors per subaperture every jth image. Moreover, pixels in the image are degraded by multiplicative noise called speckle, which makes the focusing in elevation unstable. For that reason, coherent averaging using the Singular Value Decomposition (SVD) was used. The SVD denoises and stabilizes the estimation of the phase of the signal [7]. The system model is defined as follows: given a ith stack of images, and the measured pixels Y of M by L neighboring pixels, the first singular left vector $B_i = [b_1, .., b_m]$ using the SVD can be computed. This vector keeps the information of the strongest component, which is the ground. Knowing B_i the stack of images can be calibrated per subaperture, and the compression in the third dimension, as well as the merging of all tomograms can be performed.

Now, there are two questions that have to be pointed out: how to retrieve the energy along the plane perpendicular to the line-of-sight? and how to combine the 3-D information of every ith stack? The first question is answered by two methods based on coherent averaging, beamforming (linear) and CS (nonlinear). Both methods perform compression of the energy in the third dimension per ith subaperture using all polarimetric channels (HH-VV-HV). The coordinate system is defined with respect to every middle master track of the HH polarisation, where every voxel has the coordinates (θ, r, α) (see Fig. 3).

The system can be described as $Y = AX + n$ given a ith stack, where $Y \epsilon \mathbb{C}^M$ is a complex vector of M samples for every (r, α) point, n is a complex Gaussian noise, $A \epsilon \mathbb{C}^{MxN}$

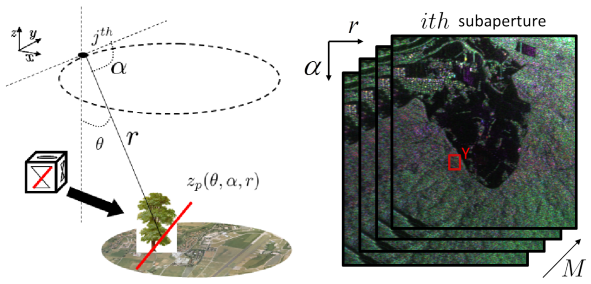

(a) CSAR 3-D geometry. (b) 2-D measurements.

Fig. 3. Circular SAR system geometry and measurements.

is the sensing matrix with (M≪N) that is determined by the flight path and $X \epsilon \mathbb{C}^N$ is the desired complex reflectivity:

$$\begin{bmatrix} y_1 \\ ... \\ y_M \end{bmatrix} = \begin{bmatrix} A_{1,1} & ... & A_{1,N} \\ ... & ... & ... \\ A_{M,1} & ... & A_{M,N} \end{bmatrix} \begin{bmatrix} x_1 \\ ... \\ x_N \end{bmatrix} + n \qquad (1)$$

In order to get accurate results the noise n of the model should be correctly estimated. As mentioned before coherent averaging stabilizes the phase. Thus the system model can be expressed as a function of the covariance matrix: $YY^\dagger = AXX^\dagger A^\dagger$, where every Y_j is a vector containing the contribution of the L neighbor pixels. The result is obtained by the diagonal of $XX^\dagger$, since it keeps the intensity of the signal that is desired to retrieve. However, due to this averaging resolution in the angular and range direction is degraded depending on the number of neighboring pixels [8]. To solve this problem, it was assumed that the diagonal of the matrix $XX^\dagger$ is sparse in space, since at P-band most of the contribution is coming from ground and just few scatterers come from the canopy.

Given $YY^\dagger$, the system model is addressed with the methods mentioned before: First, using beamforming to recover $diag(XX^\dagger)$ by an improved resolution similar to the one defined by the synthetic aperture in the vertical direction ($\sim$ 20 m). Second, using the l_1-penalized least-squares inversion of CS, also known as Basis Pursuit Denoising (BPDN) [2]:

$$\widehat{x} = arg \min_x \left\| YY^\dagger - AXX^\dagger A^\dagger \right\|_2^2 + \lambda_1 \left\| diag(XX^\dagger) \right\|_1 \qquad (2)$$

where λ_1 is a positive value that penalizes non-sparsity in the solution $\widehat{x}$. The software used to solve this minimization problem is called CVX [9].

Having $\widehat{x}$ with CS and $diag(XX^\dagger)$ in beamforming for every ith stack, the 3-D images are interpolated to a common cartesian grid (x, y, z) and combined incoherently in order to increase resolution in the (x, y) plane and reduce speckle. This model assumes that the backscattered reflectivity of the trees is anisotropic and changes as a function of the slow-time ϕ, thus having the possibility to retrieve the contribution every $10\,^\circ$ of a single image. The output of this stage are holographic tomograms per polarimetric channels, which will be combined to separate scattering mechanisms by their polarimetric signature.

4. EXPERIMENTAL RESULTS

For these experiments the size of the vecror perpendicular to the line-of-sight x was N=256 elements and M=7 due to the number of tracks. The window size for coherent averaging in range and angular direction was 3 by 5 pixels, respectively. The focused area was a forested region of 700 m by 700 m by 50 m in the center of the spotlighted region (see Fig. 2).

The following results were focused using beamforming with the covariance matrix. Fig. 4 shows the comparison of two slices of a holographic tomogram over the plane (x, y), at a given height of $z = 550$ m and using the HH channel. The image on the left depicts the contribution of a single subaperture, and the second image the addition of all aspect angles. It can be noticed that the resolution in the right image improves, because of the asymmetry in the pixel resolution. Note that more scatterers are seen in the scene, since information from different angles is added up. Targets that are at that height are focused and cone-shaped sidelobes are not present.

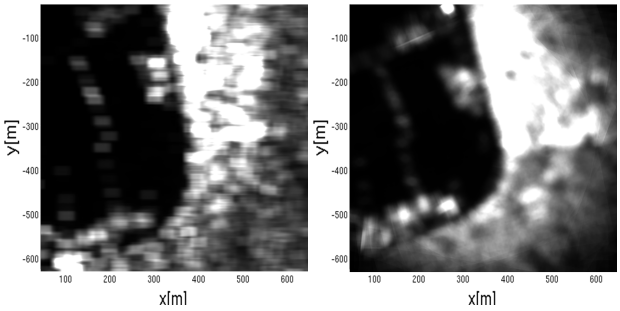

(a) Subaperture tomogram. (b) Fusion of all tomograms.

Fig. 4. Slices of the holographic tomogram in the plane (x, y) at $z = 555$ m.

It is possible to distinguish the canopy from the ground by combining the polarimetric information of all three polarimetric holograms, as shown in Fig. 5. The ground topography of the forested area can also be retrieved, giving the possibility to use it as a DEM to refocus the 2-D high resolution images. Besides the estimation of the tree height, the holographic tomography allows the estimation of the tree profile, extinction factor and 3-D signature profile, which are of high interest for the scientific community in biosphere research.

On the other hand, results using compressive sensing present a sharper retrieval of the signal as shown in Fig. 6. As expected results in the channels HH and VV give more

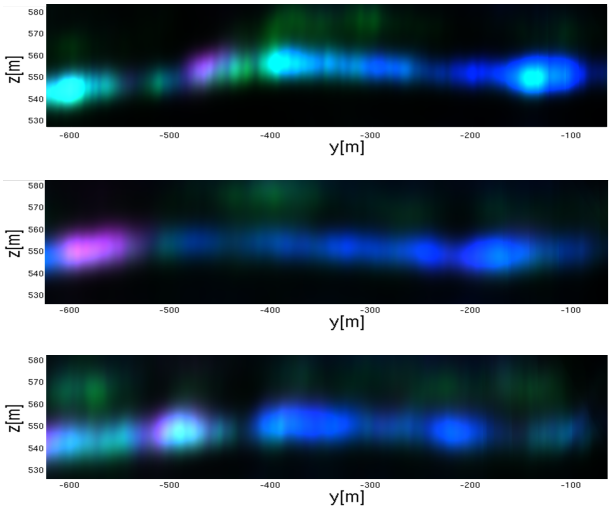

Fig. 5. Three different profiles of fully polarimetric holographic tomograms at P-Band, lexicographic basis, regular cartesian coordinates, beamforming inversion.

information about the ground, whereas HV has also a strong contribution from the canopies. The color map is a function of the height.

5. CONCLUSIONS

This work presents the first fully polarimetric multicircular SAR holographic tomograms at P-band of forested areas. It was seen that the proposed calibration method is a key factor when focusing in CSAR mode, and allows to correct constant phase offsets for each subaperture and track. This paper gives a solution on how to improve resolution in the direction perpendicular to the line-of-sight with a vertical synthetic aperture and using coherent averaging with Fourier and sparse reconstruction techniques. Every subaperture tomogram was combined incoherently to increase the resolution in the (x, y) plane, to reduce speckle and to retrieve more components in the height direction of a forested area. Future work will be focused on enhancing the holographic tomograms in a coherent manner over 360° of all circular passes, in order to achieve the theoretical resolution of $\sim \lambda/4$ on the plane (x, y), as well as high resolution in height of forested areas.

6. REFERENCES

[1] O. Ponce, P. Prats, M. Rodriguez-Cassola, R. Scheiber, and A. Reigber, "Processing of circular trajectories with fast factorized back-projection," in *Geoscience and Remote Sensing Symposium, 2011 IEEE International, IGARSS 2011*, 2011, pp. 3692 – 3695.

[2] M. Ferrara, J.A. Jackson, and C. Austin, "Enhancement of multi-pass 3D circular SAR images using sparse reconstruction techniques," in *Algorithms for Synthetic Aperture Radar Imagery XVI*, E. G. Zelnio and F. D. Garber, Eds., Orlando, FL., April 13–17 2009, SPIE Defense and Security Symposium.

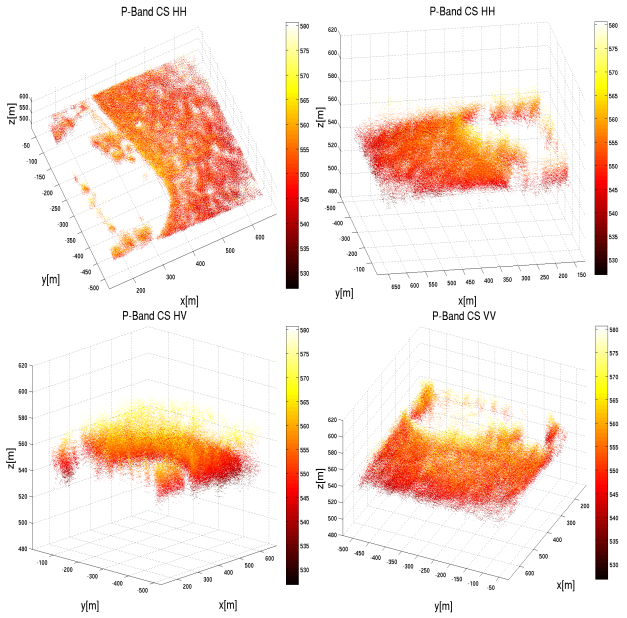

Fig. 6. Holographic tomograms at P-band, different polarisations, regular cartesian coordinates, CS inversion with $\lambda_1 = 0.5$.

[3] S. K. Shan and J. R. S. Colin, "Image formation in holographic tomography: high-aperture imaging conditions," in *Applied Optics*, 2009.

[4] A. Reigber and A. Moreira, "First Demonstration of Airborne SAR Tomography Using Multibaseline L-Band Data," in *IEEE Transactions on Geoscience and Remote Sensing*, Sep 2000.

[5] O. Ponce, P. Prats, R. Scheiber, A. Reigber, and A. Moreira, "Multibaseline 3-D Circular SAR Imaging at L-band," in *European Conference on Synthetic Aperture Radar (EUSAR)*, April 2012.

[6] Joachim H. G. Ender, "Autofocusing ISAR Images via Sparse Representation," in *European Conference on Synthetic Aperture Radar (EUSAR)*, April 2012.

[7] E. Aguilera, M. Nannini, and A. Reigber, "Multi-signal compressed sensing for polarimetric SAR tomography," in *IEEE Geoscience and Remote Sensing Symposium, 2011, IGARSS*, July 2011.

[8] E. Aguilera, M. Nannini, and A. Reigber, "Wavelet-Based Compressed Sensing for SAR Tomography of Forested Areas," in *European Conference on Synthetic Aperture Radar (EUSAR)*, April 2012.

[9] M. Grant and S. Boyd, "Graph implementations for nonsmooth convex programs," in *Recent Advances in Learning and Control*, V. Blondel, S. Boyd, and H. Kimura, Eds., Lecture Notes in Control and Information Sciences, pp. 95–110. Springer-Verlag Limited, 2008.